

Constraining new coloured matter from the ratio of 3- to 2-jets cross sections at the LHC

Diego Becciolini,^a Marc Gillioz,^a Marco Nardecchia,^{b,c} Francesco Sannino,^a Michael Spannowsky^d

^a*CP³-Origins & DIAS, University of Southern Denmark, Campusvej 55,
5230 Odense M, Denmark*

^b*DAMTP, University of Cambridge, Wilberforce Road,
Cambridge CB3 0WA, United Kingdom*

^c*Cavendish Laboratory, University of Cambridge, JJ Thomson Avenue,
Cambridge CB3 0HE, United Kingdom*

^d*Institute for Particle Physics Phenomenology, Department of Physics,
Durham University, DH1 3LE, United Kingdom*

E-mail: becciolini@cp3.dias.sdu.dk, gillioz@cp3.dias.sdu.dk,
m.nardecchia@damtp.cam.ac.uk, sannino@cp3.dias.sdu.dk,
michael.spannowsky@durham.ac.uk

ABSTRACT: The Large Hadron Collider experiments are testing the evolution of the strong coupling α_s up to the TeV scale. We show that the ratio of 3- to 2-jets cross sections provides a good determination of α_s , even in the presence of new physics. The experimental measurements can then be used to place a model-independent bound on new particles carrying QCD colour charge and can constrain such states to be heavier than a few hundred GeVs.

1 Introduction

So far the most relevant result obtained from the Large Hadron Collider has been the discovery of the Higgs boson [1, 2], however non-Higgs analyses are also very valuable. For example in [3] the first determination of $\alpha_s(M_Z)$ from measurements of momentum scales beyond 0.6 TeV was presented. This determination has been performed studying the behaviour of the ratio R_{32} of the inclusive 3-jet cross section to the 2-jet cross section, defined in greater detail in the next section. The result is in agreement with the world average value of $\alpha_s(M_Z)$.

In this paper, we argue that it is possible to constrain the presence of new coloured states using such a measurement. At the moment we are not able to perform a complete study and to put rigorous bounds on new physics. This is mainly due to fact that some relevant details (such as the complete uncertainties on the different measurements and their correlations) are not reported in [3]. Despite this difficulty, in this work we highlight the potential of such an observable and we discuss relevant aspects related to the presence of new (coloured) particles. We will show that the main effects of the new physics on R_{32} comes from the modification of the value of $\alpha_s(Q)$, thus it is possible to put lower bounds of several hundred GeV on the mass of new coloured states. In this way we are able to provide bounds relying, to a good approximation, only on the colour quantum numbers and the masses of the new particles. Another virtue of this observable is that it is sensitive to the total amount of coloured states in a specific theory. This approach provides complementary information with respect to bounds on new physics obtained from direct searches, where several assumptions have to be made in order to specify production and decay of a given particle. For instance if the new particles have the right quantum numbers, searches for di-jet resonances are particularly constraining [4], while there are models evading these bounds for which the results we present here may be relevant [5].

Efforts to constraint light coloured states in the same spirit as the present work have already appeared. For example in [6, 7] the authors considered the effect of a gluino-like state on the global analysis of scattering hadron data or in [8] where model-independent bounds on new coloured particles are derived using event shape data from the LEP experiments. Thanks to the new data from the LHC we show that an improvement of nearly one order of magnitude can be derived with respect to these works. Finally, this type of approach generalises to other sectors of the Standard Model, and the electroweak sector could for instance be constrained from high energy measurements of Drell-Yan [9].

The paper is organized as follows: in Section 2 we present the observable R_{32} and the main results obtained from [3], in Section 3 we analyse the effects of new physics, in Section 4 we present a series of expected bounds for different scenarios while in Section 5 we offer our conclusions.

2 The R_{32} observable

Considering that we wish to test quantum chromodynamics (QCD) at the highest possible energy scales, we are naturally interested in observables involving a low inclusive number of hard jets. Furthermore, the best way to keep under control uncertainties — both theoretical and experimental — is to look at ratios. The ideal candidate according to these criteria is the ratio of 3- to 2-jets (differential) cross sections, R_{32} , which is a commonly studied quantity [3, 10–14]. In this section, we review aspects of its theoretical evaluation and argue that it is indeed a sound and solid observable in many respects, with the potential to provide model-independent bounds on hypothetical new coloured physics.

We focus on the following definition of the observable, in accordance with the latest CMS analysis [3]:

$$R_{32}(\langle p_{T1,2} \rangle) \equiv \frac{d\sigma^{n_j \geq 3}/d\langle p_{T1,2} \rangle}{d\sigma^{n_j \geq 2}/d\langle p_{T1,2} \rangle}, \quad (2.1)$$

where $\langle p_{T1,2} \rangle$ is the average transverse momentum of the two leading jets in the event,

$$\langle p_{T1,2} \rangle \equiv \frac{p_{T1} + p_{T2}}{2}. \quad (2.2)$$

Other choices are possible regarding the kinematic variable: one could use the p_T of the leading jet only, or the sum of the p_T of all the jets, or construct more complicated combinations as done for the observable N_{32} considered by the ATLAS collaboration [14]. There can be important differences between these cases, in particular for what concerns higher-order corrections, as we will mention later.

The CMS analysis we chose to follow is based on 5 fb⁻¹ of data collected at 7 TeV centre-of-mass energy [3]. Jets are defined requiring transverse momenta of at least 150 GeV and rapidities less than 2.5, using the anti- k_T algorithm [15] with size parameter $R = 0.7$ and E-recombination scheme. The factorisation and the renormalisation scales are identified with $\langle p_{T1,2} \rangle$.

The state-of-the-art computations for inclusive multijet cross sections include the next-to-leading order corrections in α_s and α_W [16–19].¹ NLO QCD corrections are implemented in NLOJET++ [22], that allows to evaluate the 3- and 2-jets cross sections at the parton-level within the Standard Model. NLOJET++ can be used to verify that many uncertainties of the individual cross sections partially cancel out in the ratio R_{32} . As investigated in some detail in the experimental analyses, the PDF uncertainty is reduced to few percent; in other words, the 3- and 2-jets cross section uncertainties are positively correlated, and there is no severe mismatch between the kinematic regions of the PDFs probed for a particular value of $\langle p_{T1,2} \rangle$ in the two

¹Recent progress making use of new unitarity-based techniques will probably allow for complete NNLO results in a near future [20, 21].

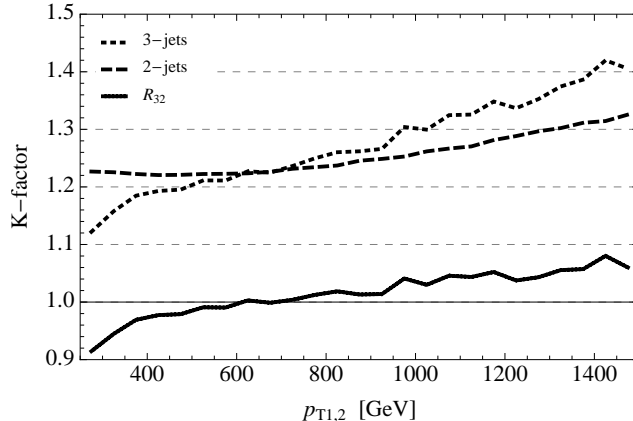


Figure 1. The NLO K -factors of the 2- and 3-jets differential cross sections and of the ratio of the two, computed with NLOJET++ [22].

cases [23]. The scale uncertainties come about in a more complicated way, as the change of factorisation and of renormalisation scales have different effects. In order to better understand the impact of higher order corrections on R_{32} , we show in Fig. 1 the relevant NLO differential K -factors, i.e.

$$K_{32}(\langle p_{T1,2} \rangle) \equiv \frac{R_{32}^{NLO}(\langle p_{T1,2} \rangle)}{R_{32}^{LO}(\langle p_{T1,2} \rangle)} \quad (2.3)$$

and similarly for the 3- and 2-jets cross sections. Since the 3- and 2-jets differential cross sections K -factor are close, the overall NLO correction to R_{32} is very much suppressed: in the kinematic range of interest, the corrections to the LO results drop from about 20 – 40% for the individual cross sections to less than about 5% for the ratio. Essentially, R_{32} has a linear dependence on α_s to a good approximation. It is not too surprising, considering that, at the squared amplitude level, the 3-jets process differs from the 2-jets process by a simple factor expressing the radiation of an extra jet [24]. This holds only for certain choices of the kinematic variable, however. Considering the ratio of differential cross sections in the leading p_T , for instance, the K -factor is very large [25]. This can be understood as a consequence of a large mismatch of kinematic configurations at LO of 2- and 3-jets events: the available phase-space in a 3-jets event where only the leading jet p_T is fixed is much more important than for a given value of $\langle p_{T1,2} \rangle$. Then, since 3-jets events are part of the NLO correction to the 2-jets cross section, it means that the 2-jets K -factor in leading p_T is significantly larger than in $\langle p_{T1,2} \rangle$, an increase that is not compensated by a similar effect in the 3-jets cross section resulting in large NLO corrections to the ratio as well. All in all, the K -factor for R_{32} is small enough so that the dependence of R_{32} on the renormalisation scale comes mainly through the change of α_s in the LO term.

We will see in the next section that the parton distribution functions of the

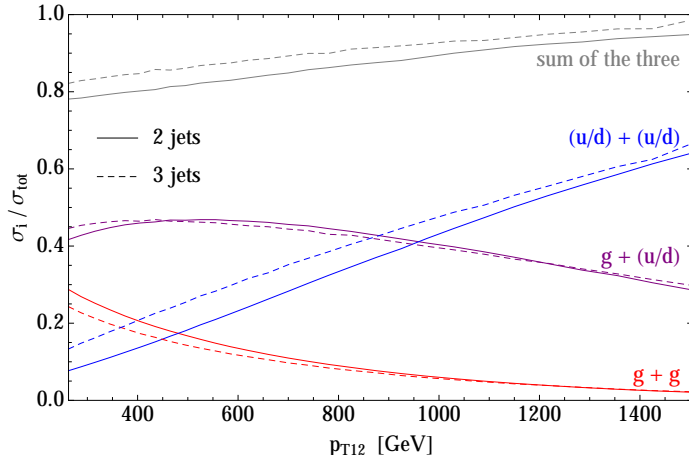


Figure 2. Relative contributions of sub-processes at LO to 2- (continuous) and 3-jets (dashed) differential cross sections, selected according to the initial-state partons: only valence quarks (blue), one valence quark and one gluon (purple), two gluons (red), the sum of these three contributions (grey).

gluon can be significantly affected by the presence of new coloured particles. It is thus instructive to describe here the relative importance of the various sub-processes that enter the parton-level cross sections, using the Standard Model as a benchmark. At higher p_T , larger values of the momentum fraction of the proton are probed, where the dominant PDFs are the ones of the valence quarks (up- and down-quarks). In Fig. 2, we show that the processes with two valence quarks in the initial state become dominant indeed, while the second most important contribution comes from processes with one valence quark and one gluon. The gluon fusion processes, as well as all other processes involving non-valence quarks, contribute little to hard events.

From our discussion in this section, it should appear that R_{32} is the ideal observable to extract values of α_s from, in the context of hadron collisions, and in that sense probably the best analogue of the R -ratio in electron-positron annihilation. It is solid against experimental uncertainties as well as theoretical ones, in particular PDF uncertainties and higher-order corrections. There is still an important ambiguity in the choice of the renormalisation and factorisation scales, which currently dominates the uncertainty [3]. These scales have to be related to the energy of the corresponding processes, however, and indeed the theoretical prediction describes the observation well only for appropriate choices.

Even though some experimental analyses do present the results of their fits in terms of the value of α_s at the energy being probed (see Fig. 3), the emphasis is on the results obtained by extrapolating back down to the usual reference scale M_Z , assuming the validity of the Standard Model (SM). The final result in the latest CMS analysis is

$$\alpha_s(M_Z) = 0.1148 \pm 0.0014 (\text{exp.}) \pm 0.0018 (\text{PDF}) \pm 0.0050 (\text{theory}), \quad (2.4)$$

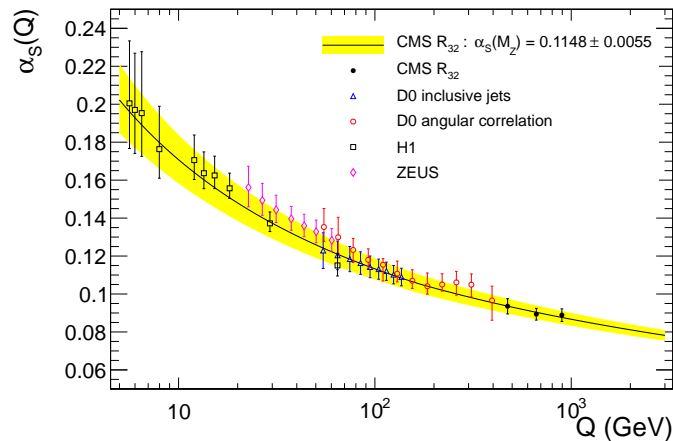


Figure 3. α_s measured at different energy scales and compared to the running obtained in the standard model. This figure is taken from [3].

and we see that the theoretical error is indeed the dominant one. We take here a different approach and argue that bounds on potential new physics beyond the SM (BSM) can be derived from such measurements.

3 R_{32} in the presence of new physics

In this section, we discuss how hypothetical new coloured particles can contribute to R_{32} . This can happen through a modification of the running of α_s and of the PDFs, and as additional contributions to the partonic cross section at leading or next-to-leading order. We argue that the most important of these effects is the change in α_s and that the determination of the strong coupling from R_{32} is thus generally reliable, even in the presence of new physics.

3.1 Running of α_s

In the presence of new coloured fermions, the running of α_s at high energy is modified compared to the Standard Model, manifested by the introduction of new coefficients in the β function. If we denote

$$\beta(\alpha_s) \equiv \mu \frac{\partial \alpha_s}{\partial \mu} = -\frac{\alpha_s^2}{2\pi} \left(b_0 + \frac{\alpha_s}{4\pi} b_1 + \dots \right), \quad (3.1)$$

then the coefficients b_0 and b_1 in any mass-independent renormalisation scheme read

$$b_0 = 11 - \frac{2}{3}n_f - \frac{4}{3}n_X T_X, \quad (3.2)$$

$$b_1 = 102 - \frac{38}{3}n_f - 20n_X T_X \left(1 + \frac{C_X}{5} \right), \quad (3.3)$$

where n_f is the number of quark flavours (i.e. $n_f = 6$ at scales $Q > m_t$), n_X the number of new (Dirac) fermions, and T_X and C_X group theoretical factors depending in which representation of the colour group the new fermions transform. One has respectively for the fundamental (dimension 3), adjoint (8), two-index symmetric (6) and three-index symmetric (10) representations,

$$\begin{aligned} T_{\mathbf{3}} &= \frac{1}{2}, & T_{\mathbf{8}} &= 3, & T_{\mathbf{6}} &= \frac{5}{2}, & T_{\mathbf{10}} &= \frac{15}{2}, \\ C_{\mathbf{3}} &= \frac{4}{3}, & C_{\mathbf{8}} &= 3, & C_{\mathbf{6}} &= \frac{10}{3}, & C_{\mathbf{10}} &= 6. \end{aligned} \tag{3.4}$$

Higher-dimensional representations have typically larger values of T_X and C_X , but will not be considered further in this work. The case of fermions in the adjoint representation — like the gluino in the MSSM — is special, since the representation is real: a Majorana mass term can be written for a single Weyl fermion, and n_X can take half-integer values. At leading order, the modification in the running of α_s only depends on a single parameter $n_{\text{eff}} \equiv 2n_X T_X$, counting the effective number of new fermions. Explicitly, we have

$$n_{\text{eff}} = n_{\mathbf{3} \oplus \bar{\mathbf{3}}} + 3 n_{\mathbf{8}} + 5 n_{\mathbf{6} \oplus \bar{\mathbf{6}}} + 15 n_{\mathbf{10} \oplus \bar{\mathbf{10}}}, \tag{3.5}$$

where $n_{\mathbf{3} \oplus \bar{\mathbf{3}}}$, $n_{\mathbf{6} \oplus \bar{\mathbf{6}}}$ and $n_{\mathbf{10} \oplus \bar{\mathbf{10}}}$ are the number of new Dirac fermions in the triplet, sextet and decuplet representations respectively, and $n_{\mathbf{8}}$ the number of Weyl fermions in the adjoint representation. Asymptotic freedom is lost for $n_{\text{eff}} > 10.5$. We do not restrict ourselves to asymptotically free theories.

Furthermore, one Dirac fermion corresponds to four complex scalar degrees of freedom; scalar particles in the spectrum thus contribute to n_{eff} four times less than corresponding Dirac fermions. For instance, the full content of the Minimal Supersymmetric Standard Model (1 adjoint Weyl fermion and 12 fundamental complex scalars) counts as $n_{\text{eff}} = 6$.

Beyond leading order, n_{eff} is not sufficient to parametrise the effect of new physics and the detailed properties of the additional particles enter the computation. The value of the Casimir (3.4) matters, but not only: since QCD is not a theory in isolation, the evolution of α_s is coupled to the other sectors, and thus other couplings of the new particles also have an influence; see for instance [26]. However, since this model-dependence comes about as a sub-leading effect, a simple description in terms of n_{eff} is a useful approximation. The importance of these effects can be evaluated by varying the value of the Casimir; we do not generically expect the influence of the other sectors of the theory to bring larger changes than this.

The running of α_s as given by the β function above is only valid at energies larger than the mass of the new coloured fermions — for simplicity, we assume that they all have the same mass m_X and that they are heavier than the top quark. Following the standard procedure, we choose to perform the matching of α_s between the high-energy regime and the effective theory without the new fermions exactly at the mass

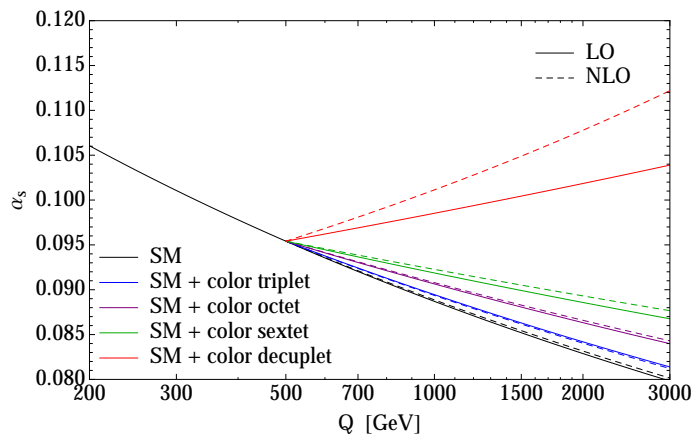


Figure 4. Example of the change in α_s induced by a new fermion of mass 500 GeV in various representations of the colour gauge group. The running of α_s is performed at NLO, showing for comparison the running at LO from the mass of the new fermion.

m_X . The choice of the matching scale Q is arbitrary and the condition $Q = m_X$ is not in itself a requirement of the theory. However this choice leads to approximate continuity of the running coupling constant and hence a more appealing physical picture of α_s (see for example [27]).

The relative importance of the change in α_s induced by fermions in various representation can be assessed from Fig. 4. With the exception of colour-decuplet fermions, the modified running of α_s is well estimated by the leading order running, which will allow us to provide model-independent bounds on new physics depending on n_{eff} and m_X only.

LHC observables can only be sensitive to scales of a few TeV at most, and since we assume in our analysis that $m_X > m_t$, the modified running of α_s will not take place over many orders of magnitude and we can derive the following approximate expression, which will be useful later in our discussion:

$$\frac{\alpha_s(Q)}{\alpha_s^{SM}(Q)} \approx 1 + \frac{n_{\text{eff}}}{3\pi} \alpha_s(m_X) \log \left(\frac{Q}{m_X} \right), \quad \text{for } Q \geq m_X, \quad (3.6)$$

where $\alpha_s^{SM}(Q)$ is the Standard Model value of the running coupling.

3.2 Parton distribution functions

New coloured fermions also affect the parton distribution functions (PDFs), besides the QCD processes at the level of the parton interactions and through the modified running of α_s . On one hand, their presence modifies the evolution of the PDFs of the quarks and gluons. On the other hand, they contribute as new partons to the momentum of the colliding protons. We will show here that in the case of R_{32} , the modifications of PDFs can actually be neglected. In order to assess the importance

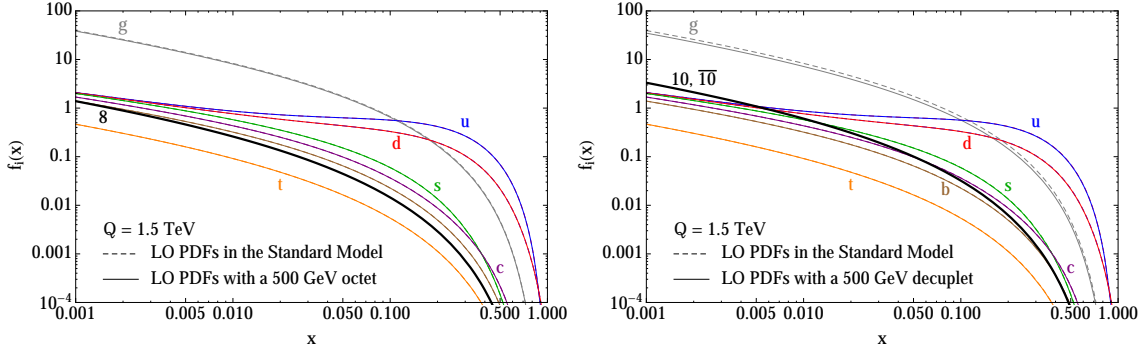


Figure 5. Relative importance of the PDFs with a new coloured fermion of mass 500 GeV in the adjoint (left panel) or three-index symmetric representation (right panel). The PDF are shown at the scale $Q = 1.5$ TeV. The Standard Model PDFs are shown in comparison as dashed lines (not visible on the left panel since the discrepancy is tiny).

of new physics effects, we make use of a modified version of HOPPET [28] to study the evolution of the PDFs above the scale of new physics. For simplicity, the evolution is performed using the DGLAP equations at leading order only and then compared to the PDFs in the Standard Model evaluated at the same order. This gives a good estimate of the modifications induced by the new fermions. The explicit procedure followed is to initialise the PDFs at the scale $Q = m_t$ with the CTEQ distribution [29], then use the DGLAP equations (A.2) of Appendix A to perform the evolution above this energy.² The results can be summarised in three points:

1. The evolution of the PDF of the new fermions above the mass threshold is driven by the gluon PDF, and it is therefore proportional to the splitting function $P_{Xg} \propto T_X$. Fermions in low-dimensional representations will therefore have a small PDF, at most comparable to that of the top quark. Fermions in a higher-dimensional representation of the colour group will have PDFs increasing faster with energy, yet they remain small compared to the valence quarks and gluon PDFs over a large range of energies. As an example, Fig. 5 shows the PDFs of a new fermion of mass $m_X = 500$ GeV in the octet (left panel) and decuplet (right panel) representations, at factorisation scale $Q = 1.5$ TeV. Although the PDF of the new fermion becomes as important as that of the light quarks, it is still one or two order of magnitude below the relevant PDFs, i.e. the valence quarks and/or the gluon ones depending on which kinematic region is considered.
2. The evolution of the gluon PDF is also largely dominated by the gluon PDF

²In principle we could use the SM PDFs up to the mass m_X of the new fermions. However, the CTEQ PDF set (like most others sets) does not make use of the 6 flavours running scheme above the top mass.

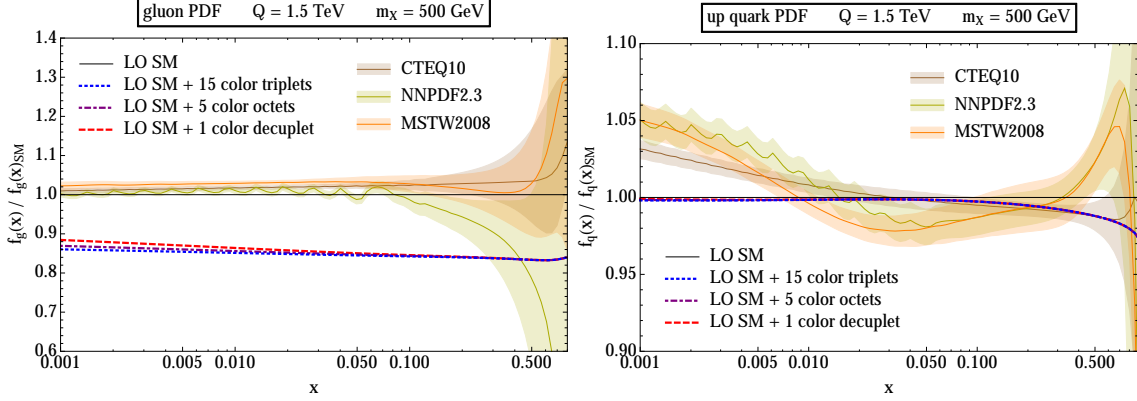


Figure 6. Change in the PDF of the gluon (left panel) and of the up quark (right panel) at $Q = 1.5$ TeV induced by a large effective number of new fermions $n_{\text{eff}} = 15$. All PDFs are normalised to the Standard Model PDFs computed at LO, which explains the discrepancy with some of the usual PDF sets shown for comparison: CTEQ10 NNLO [29], NNPDF 2.3 [30] and MSTW2008 [31].

itself. New physics enters therefore the DGLAP equations in two ways: in the value of α_s above the mass threshold and in the splitting function of the gluon into itself, eq. (A.3). The former effect is actually subleading in α_s , since the ratio $\alpha_s(Q)/\alpha_s^{SM}(Q) - 1$ is itself proportional to α_s , see eq. (3.6). The modified splitting function of the gluon, on the contrary, gives an important contribution to the evolution of the gluon PDF. It can be quantified by looking at the evolution of the ratio of the gluon PDF in the presence of new fermions to its counterpart in the Standard Model. One finds, at leading order in α_s ,

$$Q^2 \frac{\partial}{\partial Q^2} \left(\frac{f_g(x, Q)}{f_g^{SM}(x, Q)} \right) \approx -\frac{n_{\text{eff}}}{6\pi} \alpha_s(Q) \frac{f_g(x, Q)}{f_g^{SM}(x, Q)}, \quad (3.7)$$

which can be integrated to give

$$\frac{f_g(x, Q)}{f_g^{SM}(x, Q)} \approx 1 - \frac{n_{\text{eff}}}{3\pi} \alpha_s(m_X) \log \left(\frac{Q}{m_X} \right). \quad (3.8)$$

The main effect of the presence of new fermions is therefore the reduction of the gluon PDF by a factor proportional to n_{eff} but independent of x . This behaviour is confirmed by the explicit evolution obtained with HOPPET. The left-hand side of Fig. 6 shows the leading order evolution obtained for three different cases all corresponding to $n_{\text{eff}} = 15$, where all gluon PDFs are normalised to the Standard Model. Eq. (3.8) gives in this case $f_g(x, Q) \approx 0.83 f_g^{SM}(x, Q)$, which is indeed the behaviour observed.

3. The evolution of the quark PDF is less affected than the gluon PDF, for the simple reason that the splitting functions of the quark PDFs do not depend on

the presence of new fermions. Moreover, it is indirectly feeling their presence through the modification of α_s and of the gluon PDF, but the two corrections eqs. (3.6) and (3.8) are equal and in opposite direction, so that they conspire and make the quark PDF mostly insensitive to new physics. Notice however that at large x the PDF of the valence quarks are important as well in the evolution, and for them the enhancement in α_s is not compensated, hence effectively accelerating the evolution, in this case reducing the quark PDFs at large x . This is very well visible in the right-hand side of Fig. 6, where we show the normalised PDFs of the up quark for three scenarios corresponding to $n_{\text{eff}} = 15$. It should be noted in this case that the leading order evolution of the PDFs does not match very well the standard sets using the NNLO evolution equations; however, our point here is simply to show that the quark PDFs are affected very little by the presence of new fermions, which is clear from the figure.

In general, the sizeable change in the gluon PDF could have important effects on physical observables at high factorisation scale Q . The ratio R_{32} , however, is barely sensitive to this change, since the relative contribution of the gluon-induced processes to the two and three jets differential cross section is identical, as seen in Fig. 2, and since the reduction of the gluon PDF is x -independent. At the precision level of our analysis, the modification of PDFs can thus be safely neglected.

3.3 New physics contribution to hard scattering

With our definition of R_{32} , jets in the final state are assumed to originate from a standard model parton, that is a quark or a gluon. The new coloured fermions would of course also be produced copiously above the kinematic threshold, but we expect them to give a characteristic signature in the detectors. We do not study this case here, as it depends heavily on the couplings of the new fermions to standard matter, and is therefore model dependent. Notice that if it is stable, a new, heavy fermion in the final state could in principle be misidentified as a jet, since it would hadronize and end its path somewhere in the detector. There are however stringent constraints on the existence of such bound states [32]. The only processes involving new physics at tree level are therefore those with a heavy fermion and a heavy antifermion in the initial state, as for instance in the diagram of Fig. 7 (a). In spite of the possible enhancement of such processes due to large colour factors, they remain negligible due to the minor importance of the PDF of the heavy fermion.

In the absence of new diagrams compared to the standard model, the leading order effect of new physics in the two and three jets cross sections comes entirely from the modified running of α_s described above. Assuming that the choice of renormalisation scale is appropriate when considering the average p_T of the two hardest jets, α_s can be factored out of the differential observable R_{32} , such that the

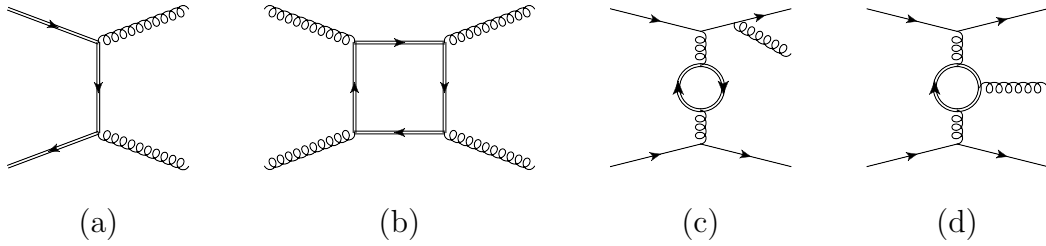


Figure 7. Some typical new physics diagrams entering the parton-level computation of two and three jets cross sections. The new, heavy fermions are denoted by a double line, the standard model ones by a single line.

new physics effects are described by

$$\left. \frac{R_{32}^{NP}(\langle p_{T1,2} \rangle)}{R_{32}^{SM}(\langle p_{T1,2} \rangle)} \right|_{LO} = \frac{\alpha_s^{NP}(\langle p_{T1,2} \rangle)}{\alpha_s^{SM}(\langle p_{T1,2} \rangle)}. \quad (3.9)$$

As discussed above, radiative corrections to R_{32} are subdominant in the standard model, and so are they in the presence of new physics. The existence of loop diagrams involving new fermions introduces a new scale in the process at the loop level, and moreover the colour factors can be enhanced in the case of fermions in a higher-dimensional representation; however, this dependence is made marginal in taking the ratio of 3 to 2 jets cross sections. In the absence of an explicit NLO computation with massive fermions, our claim is that eq. (3.9) provides a satisfactory description of new physics effects on R_{32} .

3.4 Particle-level simulations

We show finally simulations of R_{32} at the LHC at 7 and 14 TeV of center-of-mass energy, both in the standard model and for a new physics scenario. 2- and 3-jets event samples are generated with MadGraph [33] and the CTEQ10 NNLO PDF sets [29], where the presence of new physics is simulated by an appropriate modification of the running of α_s . The parton-level results displayed in Figs. 8 and 9 match the theory prediction used in the CMS analysis [3], and similarly they agree with the data obtained after unfolding. Since the showering process of the jets is mostly sensitive to soft scales, i.e. scales far below the hard-interaction scale, and thus unaffected by the modification of α_s at high energies, we can provide as well full particle-level simulations. Following [3], we recombine the final state hadrons to $R = 0.7$ anti- k_T jets with $p_{T,j} > 150$ GeV using Fastjet. We use MLM matched [34] multijet samples showered with HERWIG++ [35], and the results are shown again in Figs. 8 and 9. The observable is significantly affected by the showering process, mostly due to the migration of 2-jet events into the 3-jet category, effectively increasing the ratio R_{32} ; the relative size of the new physics contribution seems unaffected, however. The

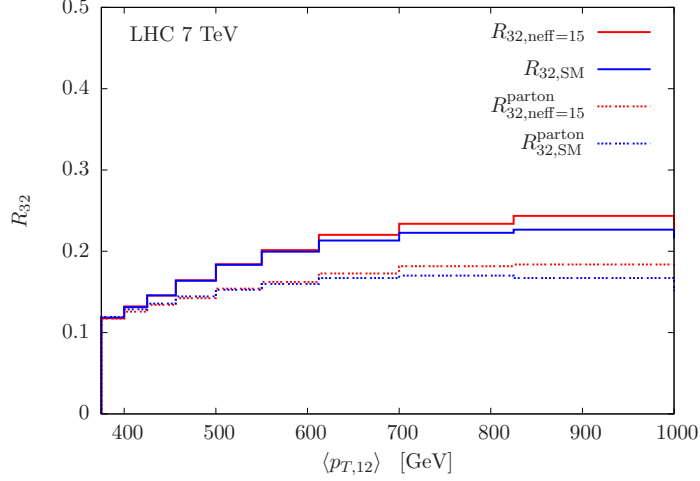


Figure 8. R_{32} at the LHC with 7 TeV of center-of-mass energy, in the standard model (blue) and for a new physics scenario with $n_{\text{eff}} = 15$ and $m_X = 500$ GeV. The dotted lines corresponds to the parton-level at leading order obtained with MadGraph [33], the solid line to R_{32} after showering with HERWIG++ [35].

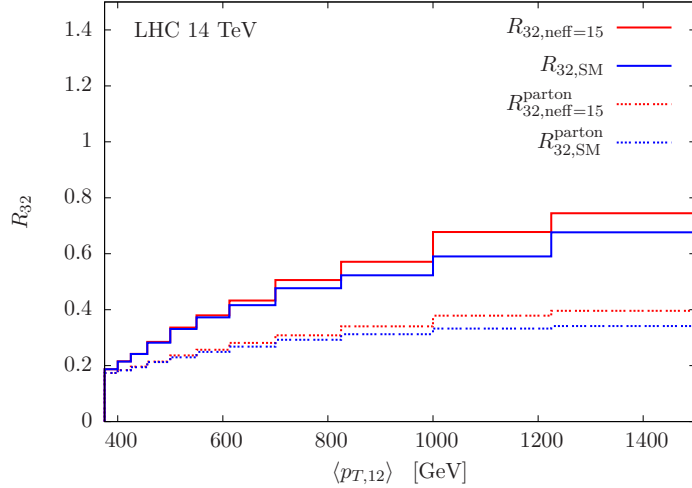


Figure 9. Same as Fig. 8 at the LHC with 14 TeV of center-of-mass energy.

CMS analysis [3] is quoting an overall systematic uncertainty due to unfolding of less than 1%. This seems challenging, given the relatively large deviations between parton-level and hardon-level, as shown in Figs. 8 and 9, and the large uncertainties in next-to-leading order parton level calculations matched to parton showers, as previously observed in studies of R_{32} [25, 36].

4 Bounds on the new physics

In the previous sections, we argued that we expect hypothetical new coloured physics to affect R_{32} principally through a modification of the running of α_s , implying that

Q [GeV]	$\alpha_s^{exp}(Q) \pm \sigma(Q)$
474	0.0936 ± 0.0041
664	0.0894 ± 0.0031
896	0.0889 ± 0.0034

Table 1: High-scale determinations of α_s from measurements of R_{32} by CMS [3].

this observable provides a robust determination of the strong coupling constant. To illustrate the exclusion potential of high-scale measurements of α_s we present bounds on n_{eff} depending on the scale of new physics m_X , derived from results provided by CMS [3]. A careful determination of these bounds would require repeating the fit to the observed values of R_{32} and precisely studying the various uncertainties. For such a complete fit, however, it is important to know how the experimental uncertainties are correlated, and this information is not provided by the collaborations.

As our goal is mainly to encourage experimental groups to also interpret their measurements in terms of exclusion bounds on new physics, we chose to perform a simplistic analysis here as a proof of concept. Motivated by the solidity of R_{32} as an observable, we take the estimates of α_s given by CMS (and reproduced in Tab. 1) at face value. We add to the analysis the world average measurement of the strong coupling $\alpha_s(M_Z) = 0.1185 \pm 0.0006$ [37]; since its uncertainty is much smaller than the ones of the other data points, we take as fixed input $\alpha_s(M_Z) = 0.1185$.

We also simply assume the uncertainties to be Gaussian and these measurements to be independent. The induced probability measure over the parameter-space we want to constrain is then simply proportional to

$$\exp \left[-\frac{1}{2} \sum_Q \left(\frac{\alpha_s^{exp}(Q) - \alpha_s^{th}(Q; n_{\text{eff}}, m_X)}{\sigma(Q)} \right)^2 \right] \times \text{priors}, \quad (4.1)$$

where $\alpha_s^{th}(Q; n_{\text{eff}}, m_X)$ is the theoretical prediction for the value of the strong coupling at the scale Q , which is a function of n_{eff} and m_X .

The theoretical predictions for α_s are obtained by running up to Q from the Z -mass at two-loop order, as described in eq. (3.1), which is sufficient for our purpose. Beyond leading-order, n_{eff} is not enough to parametrise the importance of new physics effects: the quadratic Casimir C_X needs to be specified. We vary it between 4/3 and 6 — the values corresponding to fermions in the fundamental or decuplet representations, respectively — to show that, as a subleading effect, it has little influence.

A detailed interpretation of the uncertainty on the scale of new physics m_X is beyond the scope of this analysis. We thus assume that the mass of the new states is known and show the subsequent upper bound on n_{eff} , choosing a flat prior over $n_{\text{eff}} > 0$, in Fig. 10.

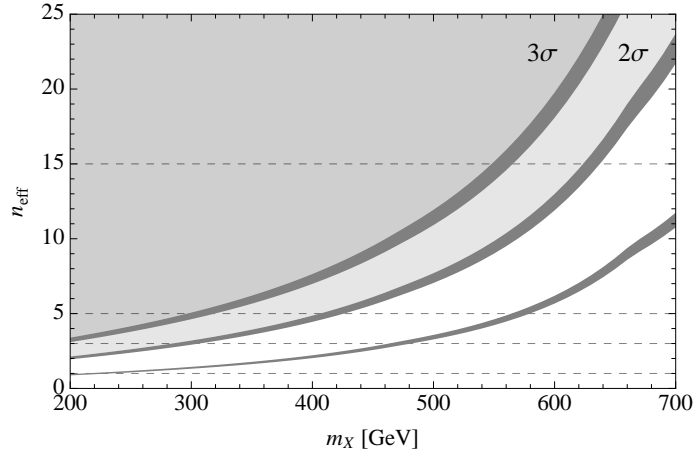


Figure 10. The shaded regions indicate the upper bounds on n_{eff} at 2σ and 3σ confidence levels, assuming the scale of new physics m_X is known. They are delimited by grey bands whose width show the effect of varying the Casimir C_X . As further indication, the third band shows a 1σ limit. To guide the eye, the dashed horizontal lines indicate values of n_{eff} corresponding to one fundamental, one adjoint, one two-index symmetric and one three-index symmetric fermion (see eq. (3.5)).

Next year, the LHC will start its second run at circa double the centre-of-mass energy, finally attaining its original target. This also means a doubling of the reach in the search for new physics: the main factors determining the number of events occurring at a given scale are the steeply falling PDFs, thus the corresponding value of the momentum fraction. Up to changes due to logarithmic scale corrections and modified experimental conditions, a same amount of data at twice the centre-of-mass energy would translate in mass-exclusion bounds roughly twice as high. Of course, all searches will see their potential increase. The relative simplicity of the analysis we suggest here may allow to extract limits on new physics rapidly as new data becomes available, though.

With the increase of collected luminosity, statistical uncertainties will shrink, which could increase the discriminating power of the search. As an example of the expected exclusion reach in the next LHC run, and of how it depends on the irreducible uncertainty, we show how fast new physics with $n_{\text{eff}} = 15$ at 500 GeV would be disfavoured against the Standard Model background hypothesis as more data will become available in Fig. 11. We estimated the limits using a binned log-likelihood CLs hypothesis test [38] based on LO evaluations of the cross sections done with NLOJET++ [22].

5 Conclusions

One should not overlook pure QCD observables as a means of placing bounds on new physics beyond the Standard Model. Such bounds can indeed be insensitive to the

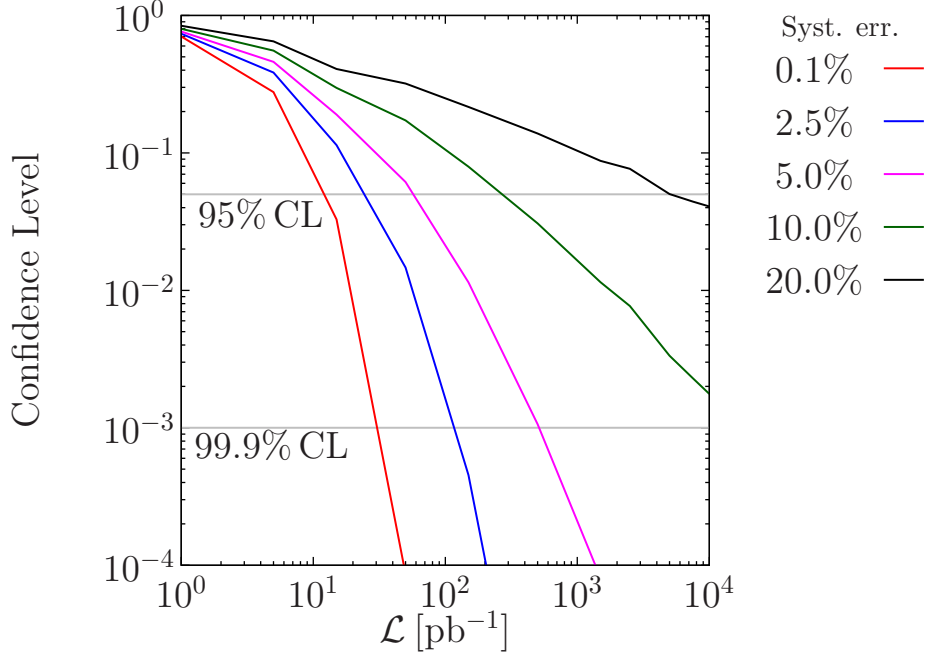


Figure 11. CLs for 14 TeV.

detailed properties of the hypothetical states, as their various charges, and mainly depend on their effective number n_{eff} (and their mass). These limits on coloured particles, although not the most stringent for any specific model in general, would be largely unavoidable due to their model-independent nature.

We show that the ratio of 3- to 2-jets inclusive differential cross sections R_{32} is particularly appropriate for constraining new physics. PDF uncertainties are suppressed, and the main effect of additional heavy particles is encoded in the modified running of the strong coupling α_s .

We encourage experimental collaborations to interpret their results not only as a test of the Standard Model, checking the compatibility with the reference value of α_s at the Z pole, but also more directly as a probe of new physics.

In order to derive robust bounds on New Physics more work has to be done. In particular a better understanding of the scale uncertainties and of the effect of showering processes should give a better idea on the sensitivity on the new coloured states. At the moment using the available information in [3] we are not able to perform such a complete analysis.

However, based on the simplified analysis on Section 4 the exclusion potential of currently available experimental data is shown in Tab. 2.

colour content	n_{eff}	m_X in GeV
Gluino	3	280
Dirac sextet	5	410
MSSM	6	450
Dirac decuplet	15	620

Table 2: 95% CL mass exclusion bounds for various values of n_{eff} according to a toy-analysis of the latest CMS measurement of R_{32} [3].

Acknowledgments

The CP³-Origins centre is partially funded by the Danish National Research Foundation, grant number DNRF90. We would like to thank Tuomas Hapola, Petar Petrov, Marek Schoenherr and the members of the Cambridge SUSY Working Group for discussions and helpful comments, as well as Olivier Mattelaer for his help with MadGraph.

A DGLAP equations with new coloured fermions

Defining the sum of the PDF of all quarks as

$$\Sigma(x, Q^2) = \sum_{q=q_i, \bar{q}_i} f_q(x, Q^2) \quad (\text{A.1})$$

and denoting by $f_X(x, Q^2)$ the PDF of the new coloured fermion — or the sum of them if they are more than one — the DGLAP evolution equations are at leading order

$$Q^2 \frac{\partial f_g}{\partial Q^2}(x, Q^2) = \frac{\alpha_s}{2\pi} \int_x^1 \frac{dz}{z} \left[P_{gg}(z) f_g\left(\frac{x}{z}, Q^2\right) + P_{gq}(z) \Sigma\left(\frac{x}{z}, Q^2\right) + n_X(Q) P_{gX}(z) f_X\left(\frac{x}{z}, Q^2\right) \right], \quad (\text{A.2})$$

$$Q^2 \frac{\partial \Sigma}{\partial Q^2}(x, Q^2) = \frac{\alpha_s}{2\pi} \int_x^1 \frac{dz}{z} \left[P_{qq}(z) \Sigma\left(\frac{x}{z}, Q^2\right) + 2n_f(Q) P_{qg}(z) f_g\left(\frac{x}{z}, Q^2\right) \right],$$

$$Q^2 \frac{\partial f_X}{\partial Q^2}(x, Q^2) = \frac{\alpha_s}{2\pi} \int_x^1 \frac{dz}{z} \left[P_{XX}(z) f_X\left(\frac{x}{z}, Q^2\right) + \frac{n_X(Q)}{n_X} P_{Xg}(z) f_g\left(\frac{x}{z}, Q^2\right) \right],$$

where $n_f(Q)$ and $n_X(Q)$ are the number of active flavours of quarks and new fermions respectively at scale Q . The splitting functions P_{ij} are defined as

$$P_{gg}(z) = 6 \left[\frac{z}{(1-z)_+} + \frac{1-z}{z} + z(1-z) \right] + \frac{1}{2} \left(11 - \frac{2}{3} n_f(Q) - \frac{4}{3} n_X(Q) T_X \right) \delta(1-z), \quad (\text{A.3})$$

$$P_{qq}(z) = 3 \left(\frac{1+z^2}{1-z} \right)_+, \quad P_{XX}(z) = C_X \left(\frac{1+z^2}{1-z} \right)_+, \quad (\text{A.4})$$

$$P_{gq}(z) = 3 \frac{1+(1-z)^2}{z}, \quad P_{gX}(z) = C_X \frac{1+(1-z)^2}{z}, \quad (\text{A.5})$$

$$P_{qq}(z) = \frac{1}{2} [z^2 + (1-z)^2], \quad P_{Xg}(z) = T_X [z^2 + (1-z)^2], \quad (\text{A.6})$$

where the group invariants T_X and C_X are defined in Section 3.1.

References

- [1] **ATLAS** Collaboration, G. Aad et al., *Observation of a new particle in the search for the Standard Model Higgs boson with the ATLAS detector at the LHC*, *Phys.Lett. B* **716** (2012) 1–29, [[arXiv:1207.7214](#)].
- [2] **CMS** Collaboration, S. Chatrchyan et al., *Observation of a new boson at a mass of 125 GeV with the CMS experiment at the LHC*, *Phys.Lett. B* **716** (2012) 30–61, [[arXiv:1207.7235](#)].
- [3] **CMS** Collaboration, S. Chatrchyan et al., *Measurement of the ratio of the inclusive 3-jet cross section to the inclusive 2-jet cross section in pp collisions at $\sqrt{s} = 7$ TeV and first determination of the strong coupling constant in the TeV range*, *Eur.Phys.J. C* **73** (2013) 2604, [[arXiv:1304.7498](#)].
- [4] T. Han, I. Lewis, and Z. Liu, *Colored Resonant Signals at the LHC: Largest Rate and Simplest Topology*, *JHEP* **1012** (2010) 085, [[arXiv:1010.4309](#)].
- [5] J. Kubo, K. S. Lim, and M. Lindner, *Electroweak Symmetry Breaking by QCD*, [[arXiv:1403.4262](#)].
- [6] E. L. Berger, P. M. Nadolsky, F. I. Olness, and J. Pumplin, *Light gluino constituents of hadrons and a global analysis of hadron scattering data*, *Phys.Rev. D* **71** (2005) 014007, [[hep-ph/0406143](#)].
- [7] E. L. Berger, M. Guzzi, H.-L. Lai, P. M. Nadolsky, and F. I. Olness, *Constraints on color-octet fermions from a global parton distribution analysis*, *Phys.Rev. D* **82** (2010) 114023, [[arXiv:1010.4315](#)].
- [8] D. E. Kaplan and M. D. Schwartz, *Constraining Light Colored Particles with Event Shapes*, *Phys.Rev.Lett.* **101** (2008) 022002, [[arXiv:0804.2477](#)].
- [9] J. Ruderman, J. Galloway, and J. Walsh, *Running Weak Couplings at 100 TeV*, February, 2014. Workshop talk. Slides available online: <https://indico.cern.ch/event/284800/contribution/1/material/slides/0.pdf>.
- [10] **UA1** Collaboration, G. Arnison et al., *Comparison of Three Jet and Two Jet Cross-Sections in p anti-p Collisions at the CERN SPS p anti-p Collider*, *Phys.Lett. B* **158** (1985) 494.
- [11] **UA2** Collaboration, J. Appel et al., *A Study of Three Jet Events at the CERN $\bar{p}p$ Collider*, *Z.Phys. C* **30** (1986) 341.

- [12] **CDF** Collaboration, F. Abe et al., *Properties of high mass multi - jet events at the Fermilab $p\bar{p}$ collider*, *Phys.Rev.Lett.* **75** (1995) 608–612.
- [13] **D0** Collaboration, B. Abbott et al., *Ratios of multijet cross sections in $p\bar{p}$ collisions at $\sqrt{s} = 1.8$ TeV*, *Phys.Rev.Lett.* **86** (2001) 1955–1960, [[hep-ex/0009012](#)].
- [14] **ATLAS** Collaboration, *Measurement of multi-jet cross-section ratios and determination of the strong coupling constant in proton-proton collisions at $\sqrt{s}=7$ TeV with the ATLAS detector.*, .
- [15] M. Cacciari, G. P. Salam, and G. Soyez, *The Anti- $k(t)$ jet clustering algorithm*, *JHEP* **0804** (2008) 063, [[arXiv:0802.1189](#)].
- [16] S. D. Ellis, Z. Kunszt, and D. E. Soper, *Two jet production in hadron collisions at order α_s^3 in QCD*, *Phys.Rev.Lett.* **69** (1992) 1496–1499.
- [17] Z. Nagy, *Three jet cross-sections in hadron hadron collisions at next-to-leading order*, *Phys.Rev.Lett.* **88** (2002) 122003, [[hep-ph/0110315](#)].
- [18] S. Moretti, M. Nolten, and D. Ross, *Weak corrections to four-parton processes*, *Nucl.Phys.* **B759** (2006) 50–82, [[hep-ph/0606201](#)].
- [19] S. Dittmaier, A. Huss, and C. Speckner, *Weak radiative corrections to dijet production at hadron colliders*, *JHEP* **1211** (2012) 095, [[arXiv:1210.0438](#)].
- [20] A. Gehrmann-De Ridder, T. Gehrmann, E. Glover, and J. Pires, *Second order QCD corrections to jet production at hadron colliders: the all-gluon contribution*, *Phys.Rev.Lett.* **110** (2013), no. 16 162003, [[arXiv:1301.7310](#)].
- [21] J. Currie, A. Gehrmann-De Ridder, E. Glover, and J. Pires, *NNLO QCD corrections to jet production at hadron colliders from gluon scattering*, *JHEP* **1401** (2014) 110, [[arXiv:1310.3993](#)].
- [22] Z. Nagy, *Next-to-leading order calculation of three jet observables in hadron hadron collision*, *Phys.Rev.* **D68** (2003) 094002, [[hep-ph/0307268](#)].
- [23] P. M. Nadolsky, H.-L. Lai, Q.-H. Cao, J. Huston, J. Pumplin, et al., *Implications of CTEQ global analysis for collider observables*, *Phys.Rev.* **D78** (2008) 013004, [[arXiv:0802.0007](#)].
- [24] F. A. Berends, R. Kleiss, P. De Causmaecker, R. Gastmans, and T. T. Wu, *Single Bremsstrahlung Processes in Gauge Theories*, *Phys.Lett.* **B103** (1981) 124.
- [25] S. Badger, B. Biedermann, P. Uwer, and V. Yundin, *Next-to-leading order QCD corrections to five jet production at the LHC*, *Phys.Rev.* **D89** (2014) 034019, [[arXiv:1309.6585](#)].
- [26] L. N. Mihaila, J. Salomon, and M. Steinhauser, *Gauge Coupling Beta Functions in the Standard Model to Three Loops*, *Phys.Rev.Lett.* **108** (2012) 151602, [[arXiv:1201.5868](#)].
- [27] R. K. Ellis, W. J. Stirling, and B. R. Webber, *QCD and Collider Physics*, vol. 8. Cambridge University Press, 1996.

- [28] G. P. Salam and J. Rojo, *A Higher Order Perturbative Parton Evolution Toolkit (HOPPET)*, *Comput.Phys.Commun.* **180** (2009) 120–156, [[arXiv:0804.3755](#)].
- [29] J. Gao, M. Guzzi, J. Huston, H.-L. Lai, Z. Li, et al., *The CT10 NNLO Global Analysis of QCD*, [arXiv:1302.6246](#).
- [30] R. D. Ball, V. Bertone, S. Carrazza, C. S. Deans, L. Del Debbio, et al., *Parton distributions with LHC data*, *Nucl.Phys.* **B867** (2013) 244–289, [[arXiv:1207.1303](#)].
- [31] A. Martin, W. Stirling, R. Thorne, and G. Watt, *Parton distributions for the LHC*, *Eur.Phys.J.* **C63** (2009) 189–285, [[arXiv:0901.0002](#)].
- [32] **ATLAS** Collaboration, G. Aad et al., *Search for long-lived stopped R-hadrons decaying out-of-time with pp collisions using the ATLAS detector*, *Phys.Rev.* **D88** (2013) 112003, [[arXiv:1310.6584](#)].
- [33] J. Alwall, M. Herquet, F. Maltoni, O. Mattelaer, and T. Stelzer, *MadGraph 5 : Going Beyond*, *JHEP* **1106** (2011) 128, [[arXiv:1106.0522](#)].
- [34] J. Alwall, S. Hoche, F. Krauss, N. Lavesson, L. Lonnblad, et al., *Comparative study of various algorithms for the merging of parton showers and matrix elements in hadronic collisions*, *Eur.Phys.J.* **C53** (2008) 473–500, [[arXiv:0706.2569](#)].
- [35] M. Bahr, S. Gieseke, M. Gigg, D. Grellscheid, K. Hamilton, et al., *Herwig++ Physics and Manual*, *Eur.Phys.J.* **C58** (2008) 639–707, [[arXiv:0803.0883](#)].
- [36] S. Hoeche and M. Schonherr, *Uncertainties in next-to-leading order plus parton shower matched simulations of inclusive jet and dijet production*, *Phys.Rev.* **D86** (2012) 094042, [[arXiv:1208.2815](#)].
- [37] **Particle Data Group** Collaboration, J. Beringer et al., *Review of Particle Physics (RPP)*, *Phys.Rev.* **D86** (2012) 010001.
- [38] T. Junk, *Confidence level computation for combining searches with small statistics*, *Nucl.Instrum.Meth.* **A434** (1999) 435–443, [[hep-ex/9902006](#)].